Journal of Testing and Evaluation

doi:10.1520/JTE20160579 / Vol. 45 / No. 6 / November 2017 / available online at www.astm.org

Z. Sun,[1] B. Behnia,[2] W. G. Buttlar,[3] and H. Reis[4]

Assessment of Low-Temperature Cracking in Asphalt Materials Using an Acoustic Emission Approach

Manuscript received November 11, 2016; accepted for publication February 21, 2017; published online May 15, 2017.

[1] Dept. of Industrial and Enterprise Systems Engineering, Univ. of Illinois Urbana-Champaign, Champaign, IL 61801

[2] Dept. of Civil and Environmental Engineering, Western New England Univ., Springfield, MA 01119

[3] Dept. of Civil and Environmental Engineering, Univ. of Missouri, Columbia, MO 65211

[4] Dept. of Industrial and Enterprise Systems Engineering, Univ. of Illinois Urbana-Champaign, Champaign, IL 61801 (Corresponding author), e-mail: h-reis@illinois.edu

Reference

Sun, Z., Behnia, B., Buttlar, W. G., and Reis, H., "Assessment of Low-Temperature Cracking in Asphalt Materials Using an Acoustic Emission Approach," *Journal of Testing and Evaluation*, Vol. 45, No. 6, 2017, pp. 1948–1958, http://dx.doi.org/10.1520/JTE20160579. ISSN 0090-3973

ABSTRACT

An acoustic emission (AE)-based approach to evaluate low-temperature cracking susceptibility of both asphalt binders and asphalt mixtures is presented. The AE binder testing approach consists of a thin film of asphalt binder bonded to a granite substrate exposed to decreasing temperatures ranging from 20°C to −50°C. Because of the differential thermal contraction between the granite substrate and the asphalt binder, thermal cracks develop in the asphalt binder. The initiation/propagation of these thermal cracks leads to a release of mechanical elastic energy in the material, i.e., acoustic emission activity that is recorded and used in determining the embrittlement temperature of the binder material. The AE-based embrittlement temperature showed excellent correlations with thermal cracking predictions based upon the binder rheological properties. Similar results were also obtained when asphalt concrete mixture samples were exposed to temperatures ranging from 20°C to −50°C. The AE-based approach for low-temperature characterization of binders and asphalt concrete mixtures is a rapid and reliable testing method that yields results with better repeatability (lower coefficient of variation) than the traditionally used methods based upon the binder rheological properties. Current results using AE source location also indicate that the AE approach could be used to quantitative evaluate the effectiveness of rejuvenators on aged asphalt pavements.

Keywords

asphalt binder, asphalt mixtures, low-temperature cracking, acoustic emission, source location technique, embrittlement temperature, rejuvenators

Introduction

In the United States, about 96 % of the approximately 4×10^6 miles of paved roads are surfaced with asphalt, and, as a result, there is an effort to develop more-efficient maintenance of asphalt pavements. The popularity of asphalt concrete derives from the fact that it delivers a smooth, quiet surface, and can be rapidly constructed, particularly during rehabilitation, i.e., resurfacing, operations. Immediately after construction, asphalt is a remarkably tough and resilient material. This is mainly because of the fact that asphalt concrete is comprised of a highly ductile and healable matrix, i.e., asphalt binder, combined with hard aggregate particles like crushed stone, which provide stiffness and strength. However, asphalt binder ages with time, particularly near the pavement surface, which causes the binder to lose its ductility and resilience. Oxidation is one of the main mechanisms behind aging of asphalt concrete, and, hence, pavement deterioration. Oxidative hardening leads to stiffness and embrittlement of asphalt binders (see **Fig. 1**), which reduces healing capacity, and increases the rate of microcrack propagation. Furthermore, the pavement system is more prone to microcrack formation, which may coalesce into larger cracks and may begin to develop surface-initiated fatigue cracking. In addition, the brittle pavement surface will be prone to channeling cracks, such as thermal and block cracks (see **Fig. 1**). Fatigue, thermal, and block cracking lead to an exponential decline in pavement serviceability and a resulting exponential increase in maintenance costs to restore the pavement to its original condition.

Traditionally, determination of cracking temperature is based on results from the bending beam rheometer (BBR) test in accordance with the standard test methods. These methods, which are based upon the rheological properties of the binder material, are very time consuming and expensive. For a review of these traditional methods, the reader is referred to the following AASHTO standards, i.e., AASHTO TP1 [1] and AASHTO MP1A [2]. Bouldin et al. [3], Dongre et al. [4], Kim [5], Kim et al. [6], Mirza and Witczak [7], Roy and Hesp [8], Shenoy [9], and Marasteanu et al. [10] also provide valuable insight into the estimation of the low-temperature performance of asphalt materials based upon their rheological properties.

Recently, an acoustic emission (AE)-based test was developed by the authors that has been shown to be highly effective as a tool to rapidly determine the low-temperature cracking threshold (i.e., embrittlement temperature) of asphalt binders and mixtures. The test, developed under a recent NCHRP IDEA project, involves the use of acoustic emission piezoelectric sensors to listen for microcrack initiation/propagation in binder or mixture samples as they are cooled to relatively low temperatures. The interested reader is referred to Apeagyei et al. [11], Dave et al. [12], Hill et al. [13], and Behnia et al. [14,15]. The approach has a number of important applications, such as providing an alternate tool for the "rapid" characterization of the low temperature "grade" of existing and newly developed binders, e.g., bio-binders, for evaluating trial asphalt mixtures such as mixtures involving recycled materials (RAP) by Behnia et al. [14,15], recycled asphalt shingles (RAS) by Arnold et al. [16], and warm mix asphalt by Hill et al. [13] and Behnia et al. [17]. The approach allows a rapid estimation of the embrittlement temperatures of the binders and mixtures samples. Additionally, the AE-based T_{CR} estimations showed relative strong correlations with AASHTO TP1 [1] and AASHTO MP1A [2]

FIG. 1 Typical forms of cracking in asphalt pavements: (a) thermal cracking and (b) block cracking.

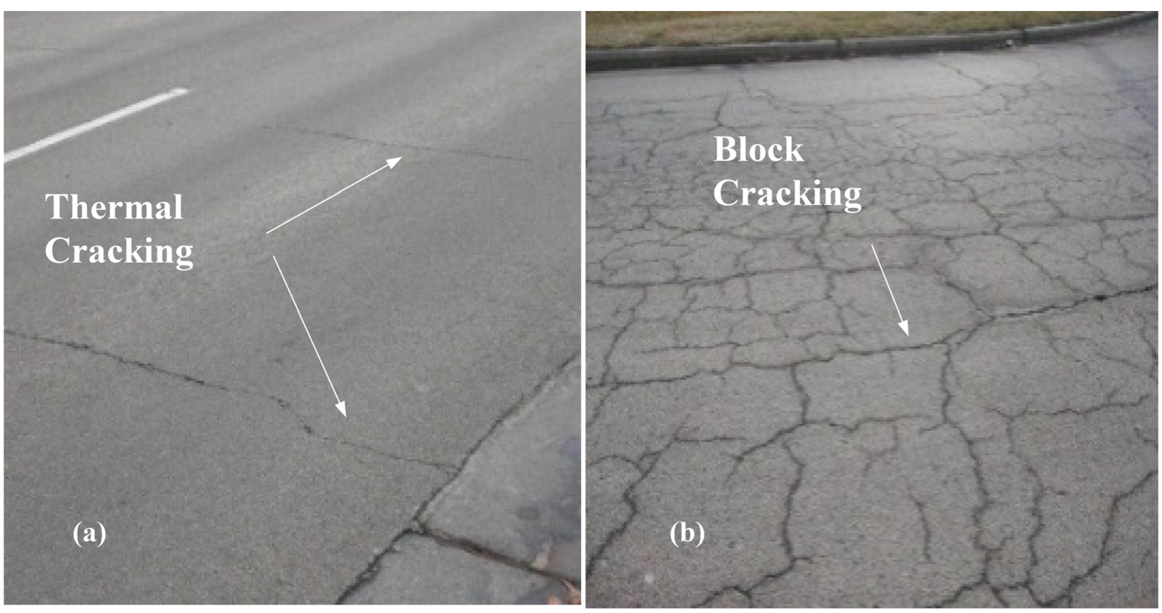

protocols and have less variability as reported by Apeagyei et al. [11] and Behnia et al. [15].

REJUVENATORS

Oxidation changes certain chemical properties of the asphalt binder; specifically, it changes its asphaltenes to maltenes ratio [11–22]. The reaction rate of oxidation can be accelerated at high temperatures and/or high exposure to ultraviolet light and air [21]. Products have also been developed to counteract the effects of oxidation. Depending on the use of the products (preventative, corrective, maintenance, or recycling), these products have been called different names such as "service life extenders," "softening agents," "rejuvenator seals," and "recycling agents/additives" [21]. For consistency, any such product is referred to as a "rejuvenator" in this study.

Rejuvenators, as the name implies, are products that aim to restore the physical and chemical properties of aged bitumen. Rejuvenators address the issue of oxidative hardening by softening the aged asphalt via the restoration of the original asphaltenes to maltenes ratio as discussed above [19,22–24]. Rejuvenators are generally applied to the surface of existing pavements; therefore, it is essential for the rejuvenator to have the ability to penetrate the surface and diffuse through the aged asphalt. If the rejuvenator lacks this ability, not only will the aged asphalt be unaffected, but the unabsorbed rejuvenator will reduce skid resistance [6,8]. To avoid creating slick, over-coated surfaces, it is often good practice to apply rejuvenators in several coats at a lower application rate [18].

Rejuvenators penetrate the pavement via capillary action and gravity, and, as a result, its penetration depends upon the pavement pore structure and tortuosity. During the diffusion process, the rejuvenator first forms a low-viscosity film around the layer of aged binder, which coats the aggregate. Then, the rejuvenator starts to diffuse into the aged binder, thus softening it. Eventually, all of the rejuvenator penetrates into the aged binder and the inner layer becomes less viscous and the outer layer becomes more viscous as the mixture approaches a state of equilibrium [23,25]. The rate of diffusion can be increased by adding diluents or by increasing temperature. Thus, the environment in which rejuvenators are applied is of critical consideration, especially in terms of application rate. After a sufficient dwell time, the performance of the rejuvenator can be evaluated. For additional reading on rejuvenators, the reader is referred to Refs [26–29].

The ability of rejuvenators to improve pavements' durability is typically evaluated by: (1) estimating the penetration by comparing the penetration at 25°C in the asphalt binder extracted from untreated and treated cores; (2) comparing the viscosity at 60°C of the asphalt binder extracted from untreated and treated cores; and (3) comparing the percentage loss of aggregate when untreated and treated samples are subjected to a pellet abrasion test [18–30]. Mainly because these tests are cumbersome and time consuming, they are not often used. There exists a need for a more reliable method for determining the effectiveness of rejuvenating agents.

In this paper, the AE-based testing approach for assessing low temperature cracking performance of both asphalt binders and asphalt mixtures is presented along with some testing results. The use of an acoustic emission source location technique to detect the location of thermal microdamage in asphalt materials is also presented. The approach is also used to evaluate the effect of rejuvenators in restoring the original embrittlement temperatures to oven-aged specimens.

Materials and Methods

In this section the specimens and methods used to evaluate binders, asphalt concrete mixtures, and the effectiveness of rejuvenators are described.

ASPHALT BINDER SAMPLES

The AE testing samples for testing asphalt binders are shown in Fig. 2. For asphalt binders, the AE sample consists of 6-mm-thick layer of asphalt binder bonded to a granite substrate. Test samples of the following binders were prepared: AAA-1 (PG 58-28), AAD-1 (PG 58-28), AAF-1 (PG 64-10), and AAG-1 (PG 58-10). In addition, three different aging levels, i.e., unaged (TANK), short-term aged (RFTO), and long-term aged (PAV) were also evaluated (see Table 1). As the temperature of the AE sample decreases, thermally induced stresses build up within the material because of the differential thermal contraction coefficients between asphalt and granite materials. Cracks occur when the thermally induced stresses equal the material strength, and are detected using acoustic emission.

ASPHALT MIXTURE SAMPLES

Asphalt concrete specimens with the same aggregate blend were prepared following Superpave guidelines. A 19 mm nominal maximum aggregate size (NMAS) with a target asphalt content of 5.9 % by weight of the total mixture was selected for this study. The PG 64-22 and PG 58-28 binders were used as the base binders (see Table 2). The aggregate blend consisted of aggregates from four different stockpiles: coarse (CM16, 65.3 %), fine (FM20, 23 %), fine (FM02, 10.5 %), and mineral filler (MF, 1.2 %). Mixing of the asphalt concrete mixtures was conducted at 155°C using a standard bucket mixing procedure. The compacted gyratory specimens were then cut to obtain the samples.

Semicircular-shaped asphalt concrete with a 50-mm thickness and a 150-mm diameter were cut and used as AE testing mixture sample (see Fig. 3). The AE asphalt mixture sample can be fabricated from either field cores or from gyratory compacted samples. To conduct the AE test, the prepared AE sample is exposed to decreasing temperatures ranging from 20°C to

FIG. 2 Acoustic emission testing of asphalt binders: (a) AE testing setup and (b) binder sample (i.e., a 6-mm-thick layer of asphalt binder bonded to granite substrate).

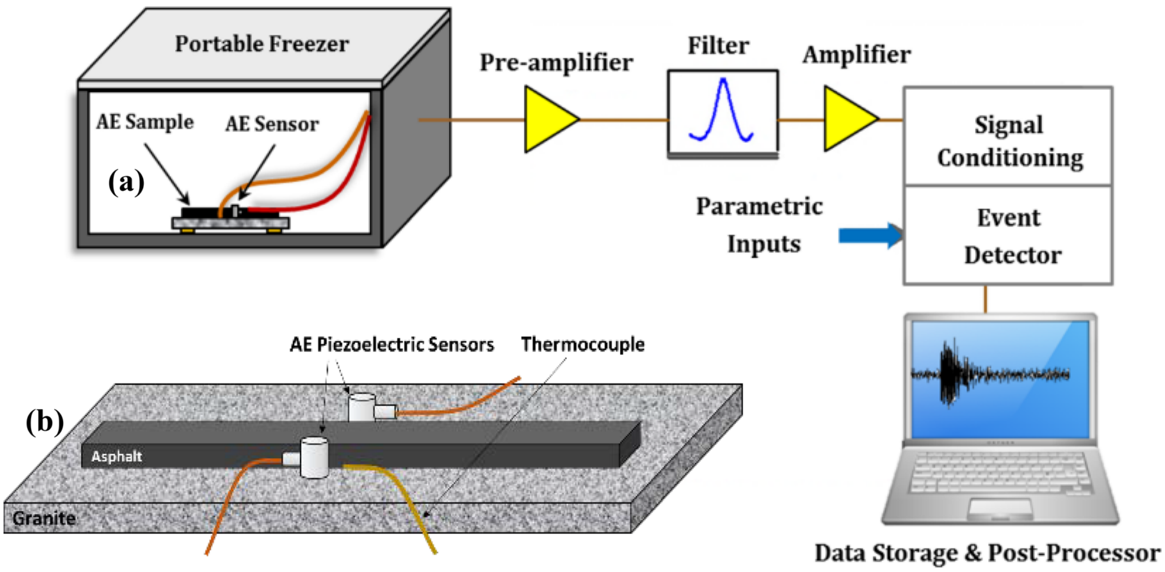

−50°C (or cooler temperatures, if needed), and the acoustic activities and temperature of asphalt material test sample is continuously monitored and recorded using piezoelectric AE sensors and a K-type thermocouple, respectively.

For asphalt mixture samples, thermally induced stresses build up because of the thermal contraction mismatch between aggregates and surrounding asphalt mastic. However, because of the larger volume there was a concern that there would be a thermal lag between the surface temperature and the temperature in the middle of the test sample. To address this concern, three thermocouples were places at different depths, i.e., at the surface, at 12 mm and at 24 mm deep inside the sample, respectively. Whereas it was observed that a significant thermal lag exists initially, it was also observed that as the temperature approaches −10°C the thermal lag is reduced to less than 0.5°C. This indicates that, at lower temperatures, relatively uniform cooling of AE test sample occurs in the portable freezer. As a result, the thermal lag at temperatures below −10°C is negligible and the temperature at the sample surface can be considered as the representative temperature of the whole specimen. Considering that acoustic emission activity of most asphalt mixtures begins at temperatures below −10°C, it can be concluded that the sample surface is an acceptable location to position thermocouples to measure the temperature of test samples during AE tests [15].

During cooling, thermal damage occurs when the thermally-induced stresses exceed the local strength of the material. Using the AE sensing system, the initiation/propagation of thermal microcracks, i.e., thermal damage, in the material is detected. The temperature corresponding to the first occurring

TABLE 1 AE-based embrittlement temperatures and BBR-based cracking temperatures of SHRP core asphalt binders.

Material	AE-Based Embrittlement Temperature T_{EMB} (°C)	AE-Based Embrittlement Temperature CoV (%)	BBR-Based Cracking Temperature (°C)
TANK-AAA1	−36.3	1.7 %	−34.5
RTFO-AAA1	−35.4	2.0 %	−32.3
PAV-AAA1	−30.9	1.9 %	−29.7
TANK-AAD1	−37.2	1.3 %	−34.4
RTFO-AAD1	−35.9	1.9 %	−33.1
PAV-AAD1	−30.6	1.5 %	−30.1
TANK-AAF1	−24.6	1.8 %	−25.4
RTFO-AAF1	−21.1	1.3 %	−24.7
PAV-AAF1	−18.7	2.6 %	−20.4
TANK-AAG1	−20.7	2.9 %	−20.0
RTFO-AAG1	−19.2	2.1 %	−19.1
PAV-AAG1	−17.2	1.5 %	−17.0

TABLE 2 Acoustic emission and disk-shaped compact tension tests results of PG64-22 and PG58-28 asphalt mixtures at different aging levels.

Material	AE Embrittlement Temperature (°C) T_{EMB}	AE Embrittlement Temperature (°C) CoV %	Fracture Energy (J/m^2) G_f	Fracture Energy (J/m^2) CoV %
TANK PG64-22	−30.28	8.9 %	486	12.3 %
RTFO PG64-22	−29.41	5.5 %	402	8.5 %
PAV PG64-22	−25.18	4.6 %	208	10.7 %
TANK PG 58-28	−36.90	6.8 %	1651	14.7 %
RTFO PG 58-28	−35.51	8.3 %	1373	9.1 %
PAV PG 58-28	−33.51	7.8 %	935	12.8 %

FIG. 3 Comparison of AE test results of asphalt mixtures versus corresponding DC(T) fracture test results: (a) AE testing of asphalt mixture sample, (b) typical temperature versus time curve for an asphalt mixture sample, (c) acoustic emission response, (d) DC(T) test sample, and (e) typical load versus crack opening displacement curve in DC(T) test. AE tests assess the material response to thermal loading at the microlevel, whereas the DC(T) tests evaluate the overall global response (i.e., at the macrolevel) of the material.

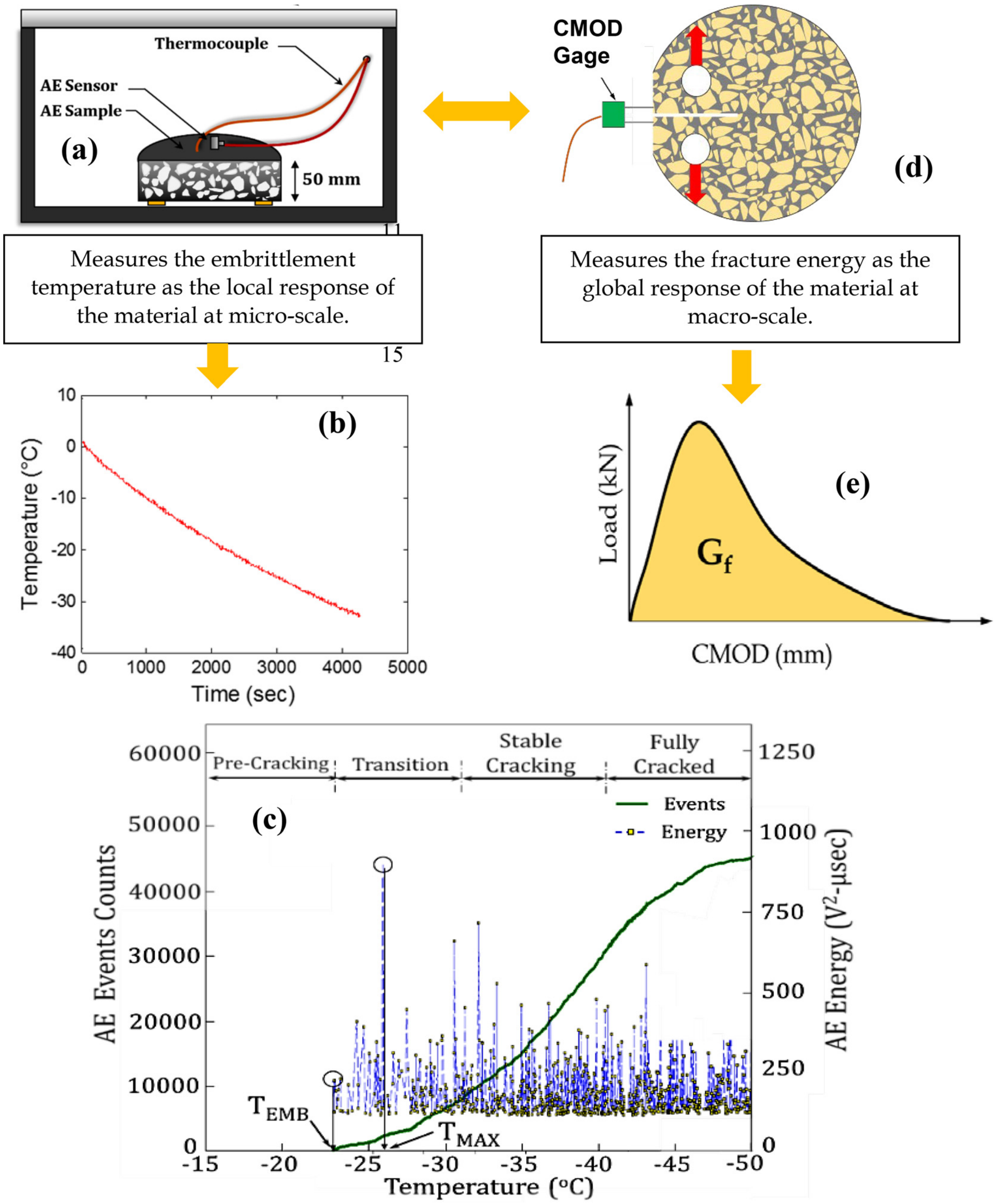

thermal damage is termed the "embrittlement temperature" of that material and is used to assess the low-temperature cracking performance of that asphalt binder or asphalt mixture. A schematic representation of the AE set up for testing asphalt mixtures is shown in **Fig. 3**, which shows the ULT-25 portable freezer along with the used wideband AE sensors with a nominal frequency range of 50 to 1.5 MHz. High-vacuum grease was used to couple the sensors to the AE test sample. Additional information regarding the experimental setup is provided by Behnia et al. [15]. **Fig. 3** also shows a typical temperature versus time curve for the asphalt mixture sample.

Analysis of the acoustic emission activity of the samples is performed on the recorded AE events signals and their associated recorded temperatures. Thermal damage within the AE sample is accompanied by the release of transient mechanical elastic waves, which travel through the material and can be picked up by AE sensors. Here, an AE event is referred to a local material change generating an AE signal with peak voltage and energy equal to or greater than 0.1 V and 4 $V^2 \cdot \mu s$, respectively, where energy is defined as the integral of the voltage squared over the duration of the waveform, i.e., event. Please see Eq 1, where t and $V(t)$ = the time and the recorded voltage, respectively,

$$AE_{\text{Energy}} = \int V^2(t)dt \tag{1}$$

To minimize the amount of extraneous data, including electronic noise, the piezoelectric AE sensors were conditioned in the cooling chamber prior to starting the test. In addition, all AE events with energy lower than 4 $V^2 \cdot \mu s$ were filtered out. All results presented in this paper are based on the above filtering procedures.

The temperature corresponding to the event with the first peak energy level equal to or larger than 4 $V^2 \cdot \mu s$ has been termed the "embrittlement temperature." It is hypothesized that the embrittlement temperature represents a fundamental material state, which is independent of material constraint and sample size (as long as a statistically representative volume is used).

DISC-SHAPED COMPACT TENSION TESTING

For comparison, asphalt mixtures were also prepared using the same asphalt binders at three different aging levels—Tank (i.e., unaged), RTFO (i.e., short-term aged), and PAV (i.e., long-term aged)—and tested using the disk-shaped compact tension [DC(T)] testing method (ASTM D7313-13 [31]) (see **Table 2**). The DC(T) test method is a recognized mechanical performance test, commonly used to evaluate the thermal cracking performance of asphalt mixtures. The DC(T) test methods was performed to evaluate the corresponding fracture energies [31,32] (see **Fig. 3**).

OXIDIZED SAMPLES TREATED WITH REJUVENATORS

Here, the AE source location technique using the Geiger's method [33] was implemented to determine the precise location of thermal damage within asphalt mixtures. This AE approach was implemented on PG64-22 mixture at different aging levels, i.e., unaged samples and aged samples. The aged samples were prepared in the laboratory by placing the loose uncompacted PG64-22 mixture in the force draft oven set at 135°C for 36 h. To ensure uniform aging throughout the sample, the mixtures were hand-stirred every 12 h. Following Braham et al. [32], the accelerated oven-aging process was performed to achieve high oxidative aging level in a reasonably short amount of time. In addition to evaluating the effectiveness of the rejuvenator, 36-h oven-aged samples were treated with rejuvenator by spreading a thin layer of rejuvenator (10 % of the binder by weight) on the specimen top plane surface, and performing the AE test after a 2-week dwell time.

Geiger's Source Location

The Geiger's iterative source location technique [33] was also used in conjunction with the AE-based testing method to determine the location of thermal damage within asphalt mixtures. The locations of thermally induced microcracks within asphalt materials were determined through implementation of the AE source location method using the information of the waveforms received at the AE sensors. The assumption of constant acoustic wave velocity and straight wave propagation path were made to mitigate the effect of heterogeneity, and the stochastic nature of asphalt concrete. Because the binder gets stiffer with aging, an average mixture acoustic velocity value based on the velocities reported by McGovern et al. [34] for oven-aged binders for 0, 12, 24, 28, and 36 h at 135°C was used. The Geiger's method [33] is an application of the Gauss–Newton algorithm, which is a classical algorithm for solving non-linear least-squares problems through a numerical search routine. The algorithm is called recursive because it uses the outputs from the previous run as the parameter input of the next iteration to obtain fast convergence to the solution of the unknown parameters. The Geiger's method [33] requires information from at least four sensors to build the following arrival time function at the ith sensor $f_i(x, y, z, t)$ as:

$$f_i(x, y, z, t) = T_s + \frac{1}{v}\sqrt{(x_i - X_s)^2 + (y_i - Y_s)^2 + (z_i - Z_s)^2} \tag{2}$$

where:

(X_s, Y_s, Z_s) = the spatial coordinates of the source,
(x_i, y_i, z_i) = the coordinates of the ith sensor,
v = the known acoustic wave velocity, and
T_s and t_i = the unknown source event occurring time and the known receiving time by the ith sensor, respectively.

Equation 2 is then expanded using Taylor series at a point (x_0, y_0, z_0), near the actual source. Neglecting higher-order terms, it gives:

$$f_i(x, y, z, t) = f_i(x_0, y_0, z_0, t_0) + \epsilon_i \tag{3}$$

where:

ϵ_i, the residual term, = the difference between the calculated arrival time and the observed arrival time with respect to the ith sensor:

$$\epsilon_i = \frac{\partial f_i}{\partial x}\delta x + \frac{\partial f_i}{\partial y}\delta y + \frac{\partial f_i}{\partial z}\delta z + \frac{\partial f_i}{\partial t}\delta t \tag{4}$$

The term ϵ_i, also called the correction vector, is determined using the first-order derivatives of the arrival time function. The goal of Geiger's method is to minimize the residual term ϵ_i by going through several iterations of Eq 3. The results of (x, y, z, t) of the previous iteration are substituted as (x_0, y_0, z_0, t_0) in the next iteration until ϵ_i converges to a sufficiently small threshold value. The starting trial location (x_0, y_0, z_0, t_0) is typically chosen to be the location of the sensor with the smallest observed arrival time among the four sensors, mainly because it should have the closest distance to the AE source. Generally, the trial solution $f_i(x, y, z, t)$ converges to the precise location of the damage source within 3–5 iterations. The arrival time function can diverge to an infinitely large value when the correction term keeps increasing and never meets the terminating criteria. The problem of divergence is often the result of using inaccurate arrival times as the initial input of the iterative search.

One extra step was taken during the iteration process to avoid the error induced by surface waves. If the AE source is located near the top or the bottom flat surface of the asphalt concrete specimen, some of the signals received by the sensors attached on those surfaces consisted of surface waves, which have much slower propagation velocity than the dilatational waves received by sensors on the opposite side of the specimen. To mitigate the effect of surface waves, when an initial iterative search located a source near the surface, an additional iterative search was conducted using only the information from the sensors attached on the opposite side of the specimen to update its location.

Iterative source location method provides a linear approximation of the nonlinear source location problem. By using first-order Taylor polynomials to characterize the arrival time function, Geiger's method provides an alternative approach to the conventional triangulation-based source location methods. Iterative methods are more time consuming compared to the non-iterative methods such as the one developed by Leighton and Duvall [35] at the U.S. Bureau of Mines (USBM method) mainly because the source location of each AE event has to go through several iteration processes; however, the iteration process gives more tolerance to the errors involved in the measurements because the correction term in each iteration improves the accuracy of the location results, which helps to mitigate the stochastic nature of asphalt mixtures.

Experimental Results

In this section, some acoustic emission-based results of the embrittlement temperatures of asphalt binders and asphalt mixtures are presented.

ACOUSTIC EMISSION TEST RESULTS FOR ASPHALT BINDERS

Table 1 shows the AE-based embrittlement temperatures and BBR-based cracking temperatures of SHRP core asphalt binders. The AE embrittlement temperature (T_{EMB}) of asphalt binders are compared against the critical cracking temperature (T_{CR}) obtained from the bending beam rheometer (BBR) based on Superpave asphalt binder testing procedures as described by Marasteanu et al. [10]. In all cases, a minimum of four replicates were used to produce the average values and the coefficient of variation (CoV%) of results are also presented. The COV statistic is temperature-scale dependent (different results would be obtained for results expressed in degrees Kelvin versus degrees Celsius, for example), and would produce infinite values for means approaching zero. However, for the present application, where embrittlement temperatures are in a relatively narrow range and sufficiently below zero, the COV statistic was deemed to be a useful statistical parameter to describe the repeatability of the measurements obtained. The fairly low COV% of embrittlement temperatures demonstrates the precision and good repeatability of the AE approach in testing asphalt materials. Results also show that the AE testing method is sensitive to the binder type as well as the oxidative ageing level of asphalt materials as the T_{EMB} (TANK) $<$ T_{EMB} (RTFO) $<$ T_{EMB} (PAV). In addition, comparison of AE and BBR results presented in **Fig. 4** shows that AE embrittlement temperatures have a reasonably good correlation with BBR-based cracking temperatures.

FIG. 4 Correlation between AE-based binder embrittlement temperatures and SUPERPAVE BBR-based cracking temperatures.

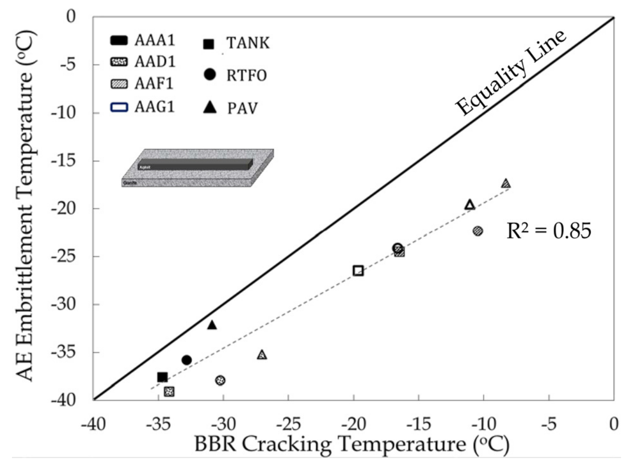

ACOUSTIC EMISSION AND DC(T) TEST RESULTS OF ASPHALT MIXTURES

Table 2 presents the AE embrittlement temperatures alongside the DC(T) fracture energies of mixtures. The AE results show that the embrittlement temperature is sensitive to the type as well as the oxidative aging level of the binder of the mixture. Regarding the type of binder, it is observed that the lower the PG low-temperature (PGLT) of the base binder of the mixture, the lower the T_{EMB} of that mixture. For the oxidative aging of the mixture, results show that the higher the aging level of the mixture, the warmer the embrittlement temperature of that mixture [T_{EMB} (TANK) $<$ T_{EMB} (RTFO) $<$ T_{EMB} (PAV)]. The overall trends of DC(T) fracture energies results are consistent with those of the AE embrittlement, as: (1) the higher the oxidative aging level, the lower the fracture resistance of the material [G_F (TANK) $>$ G_F (RTFO) $>$ G_F (PAV)], and (2) the lower the

FIG. 5

Acoustic emission (AE) source location of asphalt mixtures: (a) eight AE sensors, four sensors mounted on each side of the specimen, (b) valid AE source location distribution for a typical 36-h-aged specimen, (c) used AE source locations (clustered in the red inner cylinder with an 8-cm diameter) for estimation of embrittlement temperatures.

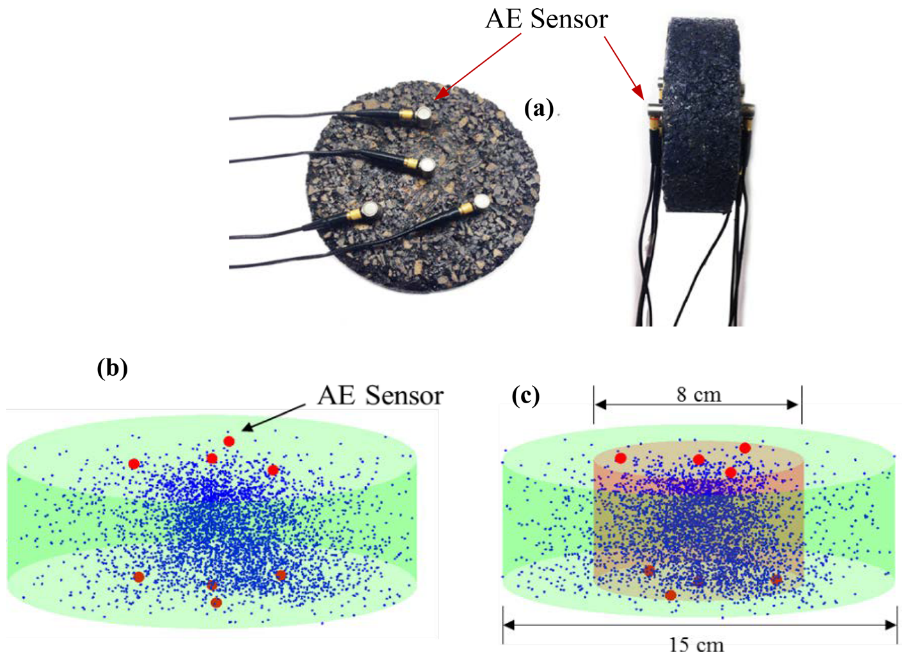

PGLT of the mixture, the higher (better) its fracture resistance [G_F (Mix PG58-28) > G_F (Mix PG64-22)]. **Fig. 3** schematically illustrates and compares the AE and DC(T) tests where DC(T) captures the global response of the material at macroscale, whereas the AE focuses on the local response of the asphalt concrete at microscale.

EMBRITTLEMENT TEMPERATURES OF OXIDIZED SPECIMENS AFTER TREATMENT WITH REJUVENATOR

As shown in **Fig. 5a**, to perform the AE source location technique, four AE piezoelectric sensors were coupled on each side of the specimen. The sensors placed at the bottom side of the specimens have 45° offset angle with respect to the sensors coupled on the top surface. The offset angle is to prevent obtaining inaccurate source location results caused by symmetric sensor placement. This sensor placement ensures a large portion of the asphalt concrete is covered within the monitoring range of the eight sensors. The valid locations of all AE sources for a typical 36-h-aged asphalt concrete specimen are displayed as dark dots in **Fig. 5b**, where it is observed that most of the AE sources are clustered in the center cylindrical region of the cylindrical asphalt specimen, as shown in **Fig. 5c** as an inner cylinder. This inner cylinder represents the valid monitoring range of the eight AE sensors placed as shown in **Fig. 5**. AE sources bounded by the inner cylinder have closer distances to all of the eight sensors, so the acoustic waves produced by these AE sources are more likely to be picked up by at least four sensors compared to the AE sources not enclosed by the inner cylinder. In addition, errors caused by reflections are likely to occur when the AE sources are located near the surrounding cylindrical boundary of the specimen. The acoustic wave mode converts and reflects at the asphalt-air boundary, which may cause false measurements of the arrival times. To mitigate these effects, only the AE sources within the red cylinder are used for the embrittlement temperature analysis. This does not affect the analysis results because only the depth of each AE source is of interest for the evaluation of the rejuvenator efficiency.

Fig. 6a shows the relationship between the height of the AE sources and their occurring times for a 36-h-aged specimen. It shows that, after the specimen was cooled for 1000 s, AE events started to occur at various heights in the specimen. The early AE events occur at the "pre-cracking region" or the early "transition region" [12–16]. At this stage, the AE events have very low energies and are randomly distributed within the specimen. As the temperature continuous to drop, the tensile thermal stresses increase within the mastic as its fracture resistance decreases; this leads to significant damage, i.e., cracking, to occur within the asphalt concrete. This stage is called the "stable cracking region," where a rapid increase in the number of AE events is observed. The embrittlement temperature is the temperature at which this stage begins. As supported by the experiments conducted in past studies, the embrittlement temperature for a 36-h aged specimen is at around −13.0°C [12–16].

In **Fig. 6a**, a rapid increase in the number of AE events is observed after about 2000 s of cooling time, where the increasing rate of AE events within a 5-mm-thick layer is higher than 10 events per 1 min. The process of finding the increasing rate of AE events at each height can be carried out by moving a 5-mm-tall and 60 s wide box (in blue) to the left until the

FIG. 6 Estimation of the embrittlement temperatures: (a) height at which the AE sources are located versus the cooling time for the 36-h-aged specimen, (b) the box (5 mm versus 1 min) is moved to the left until it encloses 10 acoustic emission events, which defines the embrittlement temperature at the centroid of the box.

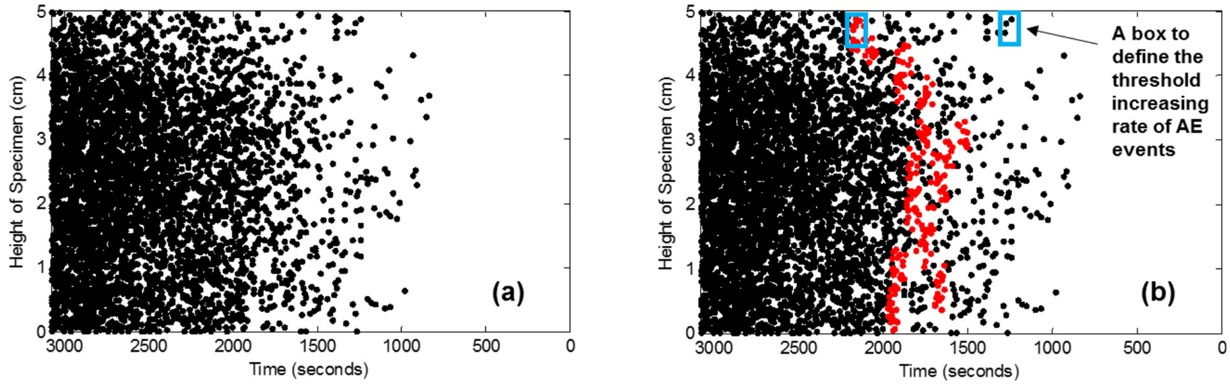

FIG. 7

Embrittlement temperatures: (a) average embrittlement temperature (dotted line) at each height interval of asphalt concrete samples oven-aged for 36 h, and (b) average embrittlement temperature (dotted line) at each height interval of the virgin asphalt specimens.

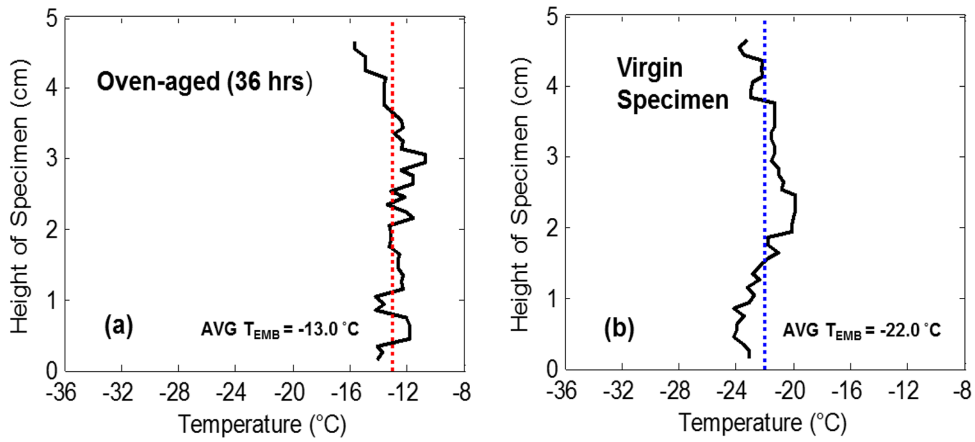

rectangular box encloses 10 AE sources (see **Fig. 6b**). **Fig. 6b** shows these enclosed AE sources, which are colored in red, and indicate the beginning of the "stable cracking region." The average occurring temperature for the AE sources enclosed in each rectangular box (in blue) was computed, and the relationship between the height of each box and the average occurring temperature of the AE sources in that box (for the 36-h aged specimen) is shown in **Fig. 7a**. For comparison, the same procedure is repeated for a virgin asphalt mixture specimen and the results are plotted in **Fig. 7b**.

Fig. 7 shows the average embrittlement temperature along the thickness of the 36-h aged specimen is −13.0°C, whereas the average embrittlement temperature for the unaged specimen is −22.0°C. The embrittlement temperature values for these two specimens are consistent with the embrittlement temperatures determined using traditional methods, which are based upon the binder's rheological properties [1–10] and with other results obtained using other acoustic emission techniques [11].

The embrittlement temperature profile of the rejuvenator-treated aged asphalt mixture is shown in **Fig. 8**. The acoustic

FIG. 8 Embrittlement temperature profile of the 36-h oven-aged asphalt mixture sample 2 weeks after being exposed to rejuvenator on the top surface. The height = 5 cm represents the top surface of the sample where a thin layer of rejuvenator (10 % of the binder by weight) was applied. The averaged embrittlement temperature (dotted line) over the thickness is shown as a dotted line.

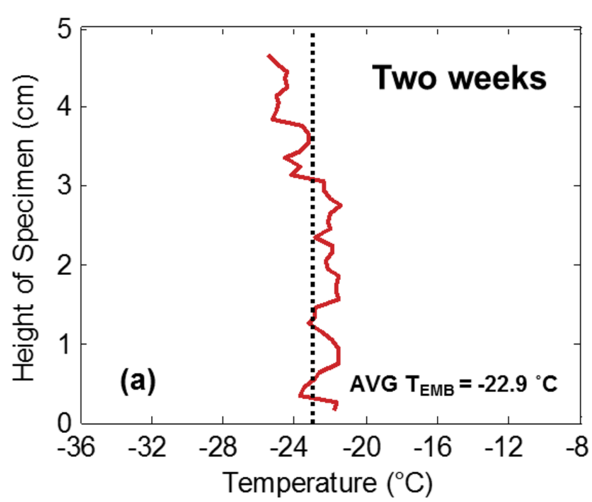

emission test was then conducted after a dwell time of 2 weeks. Results indicate that after the 2 weeks of dwell time, the embrittlement temperatures of the aged mixture have been restored to those of the unaged mixture. Examining the embrittlement temperature profile throughout the sample thickness also shows that the embrittlement temperature of the top portion of the sample (top 2 cm) is lower than the bottom portion of the sample. Because the rejuvenator permeates the specimen by gravity and capillary action, it had additional time to act upon the aged asphalt material at the top material layer of the sample. Using longer dwell times would lead to a more uniform (through the thickness) distribution of the embrittlement temperatures and possibly cooler embrittlement temperatures if excessive levels of rejuvenator were used.

Conclusions

The application of an AE-based approach to evaluate embrittlement temperatures of asphalt binders and asphalt mixtures is presented. The AE-based embrittlement temperature results of asphalt materials at different aging levels (i.e., unaged, short-term aged, and long-term aged) showed that the AE approach is sensitive to binder type as well as to the aging level of asphalt materials, i.e., the higher the aging level, the warmer the embrittlement temperature becomes. It was also observed that for both asphalt binders and asphalt mixtures the overall trends of embrittlement temperatures were consistent with those obtained from binder and mixture mechanical performance tests such as BBR and DC(T) methods. This provides additional confidence in the use of the T_{EMB} quantity as a screening tool to quickly assess the thermal cracking resistance of asphalt materials.

In addition, an iterative acoustic emission source location technique was employed to locate the source of thermal damage within the asphalt materials and to determine the through-thickness embrittlement temperature profile of virgin samples, oven-aged samples for 36 h at 135°C, and rejuvenator-treated asphalt mixture samples after being oven aged for 36 h at 135°C. Results showed that AE approach could successfully evaluate the embrittlement temperature profile of asphalt mixtures at different aging levels. Moreover, it was capable of providing a quantitative assessment of the effectiveness of the used rejuvenator.

Based on this study, it can be inferred that the AE-based test may be considered as a viable testing method for characterization of low-temperature performance of both asphalt binders and asphalt mixtures. The findings of this study also suggest that the AE-based method may provide a reliable approach to accurately determine the depth to which rejuvenators are able to penetrate, and their actual effectiveness in restoring a pavement surface to its original crack resistant state. As a result, the presented AE-based approach could potentially be used for: (1) as an evaluation tool to determine the level of pavement oxidative aging, and (2) as a laboratory design tool, to assess the effectiveness of rejuvenators in restoring the pavement surface to its crack-resistant state. Further field validation trials and standardization of the test method are underway.

ACKNOWLEDGMENTS

The writers acknowledge those who contributed to the success of NCHRP IDEA project No. 170, including the program manager, Dr. Jawed. The writers are grateful for the partial support of the U.S. Airforce Civil Engineering Center (AFCEC), including the technical support of our technical contact Dr. George Vansteenburg. The writers are also very grateful for the technical support of Dr. Jeb S. Tingle (ERDC-RDE-GSL-MS). Any opinions, findings, and conclusions or recommendations expressed in this publication are those of the authors and do not necessarily reflect the views of the sponsoring agency.

References

[1] AASHTO TP1, *Standard Specification for Determining the Flexural Creep Stiffness of Asphalt Binder Using the Bending Beam Rheometer (BBR)*, American Association of State Highway and Transportation Officials, Washington, DC, 1999.

[2] AASHTO MP1A, *Standard Specification for Determining Low-Temperature Performance Grade of Asphalt Binders*, American Association of State Highway and Transportation Officials, Washington, DC, 2001.

[3] Bouldin, M. G., Dongre, R., Rowe, G. M., Sharrock, M. J., and Anderson, D. A., "Predicting Thermal Cracking of Pavements from Binder Properties: Theoretical Basis and Field Validation," *J. Assoc. Asphalt Pavement Technol.*, Vol. 69, 2000, pp. 455–496.

[4] Dongre, R., Bouldin, M. G., Anderson, D. A., Reinke, G., D'Angelo, J., Kluttz, R. O., and Zanzotto, L., "Overview of the Development of the New Low-Temperature Binder Specification," *Technical Report*, Federal Highway Administration Binder Expert Task Group, Washington, DC, 1999.

[5] Kim, S. S., "Direct Measurement of Asphalt Binder Thermal Cracking," *J. Mater. Civil Eng.*, Vol. 17, No. 6, 2000, pp. 632–639, http://dx.doi.org/10.1061/(ASCE)0899-1561(2005)17:6(632)

[6] Kim, S. S., Wysong, Z. D., and Kovach, J., "Low-Temperature Thermal Cracking of Asphalt Binder by Asphalt Binder Cracking Device," *Transport. Res. Rec.*, Vol. 1962, 2006, pp. 28–35, http://dx.doi.org/10.3141/1962-04

[7] Mirza, M. W. and Witczak, M. W., "Development of a Global Aging System for Short Term and Long Term Aging of Asphalt Cements," *J. Assoc. Asphalt Paving Technol.*, Vol. 64, 1995, pp. 393–430.

[8] Roy, D. and Hesp, S. A. M., "Low-Temperature Binder Specification Development: Thermal Stress Restrained Specimen Testing of Asphalt Binders and Mixtures," *Transport. Res. Rec.*, Vol. 1766, No. 9, 2001, pp. 7–14, http://dx.doi.org/10.3141/1766-02

[9] Shenoy, A., "Single-Event Cracking Temperature of Asphalt Pavements Directly from Bending Beam Rheometer Data," *J. Transport. Eng.*, Vol. 128, No. 5, 2000, pp. 465–471, http://dx.doi.org/10.1061/(ASCE)0733-947X(2002)128:5(465)

[10] Marasteanu, M., Zofka, A., Turos, M., Li, X., Velasquez, R., Li, X., Williams, C., Bausano, J., Buttlar, W., Paulino, G., Braham, A., Dave, E., Ojo, J., Bahia, H., Gallistel, A., and McGraw, J., "Investigation of Low Temperature Cracking in Asphalt Pavements," *Report No. 776*, Minnesota Department of Transportation, St. Paul, MN, 2007.

[11] Apeagyei, A. K., Buttlar, W. G., and Reis, H., "Assessment of Low-Temperature Embrittlement of Asphalt Binders Using an Acoustic Emission Approach," *Insight*, Vol. 51, No. 3, 2009, pp. 129–136, http://dx.doi.org/10.1784/insi.2009.51.3.129

[12] Dave, E. V., Behnia, B., Ahmed, S., Buttlar, G. W., and Reis, H., "Low Temperature Fracture Evaluation of Asphalt Mixtures Using Mechanical Testing and Acoustic Emission Techniques," *J. Assoc. Asphalt Paving Technol.*, Vol. 80, 2011, pp. 193–226.

[13] Hill, B., Behnia, B., Hakimzadeh, S., Buttlar, W. G., and Reis, H., "Evaluation of the Low Temperature Cracking Performance of WMA Mixtures," *Transport. Res. Rec.*, Vol. 2294, 2012, pp. 81–88, http://dx.doi.org/10.3141/2294-09

[14] Behnia, B., Dave, E. V., Ahmed, S., Buttlar, W. G., and Reis, H., "Effects of Recycled Asphalt Pavement Amounts on Low Temperature Cracking Performance of Asphalt Mixtures Using Acoustic Emissions," *Transport. Res. Rec.*, Vol. 2208, 2011, pp. 64–71, http://dx.doi.org/10.3141/2208-09

[15] Behnia, B., Buttlar, W. G., and Reis, H., "An Acoustic-Emission Based Test to Determine Asphalt Binder and Mixture Embrittlement Temperature" *NCHRP-IDEA Project 144*, NCHRP IDEA Program, University of Illinois at Urbana-Champaign, Champaign, IL, 2011.

[16] Arnold, J., Behnia, B., Buttlar, W. G., and Reis, H., "Evaluation of Low-Temperature Properties of HMA Mixtures Containing Recycled Asphalt Shingles Using an Acoustic Emission Approach," *J. Construct. Build. Mater.*, Vol. 58C, 2014, pp. 1–8.

[17] Behnia, B., Buttlar, W. G., and Reis, H., "Cooling Cycle Effects on Low Temperature Cracking Characteristics of Asphalt Concrete Mixtures," *Mater. Struct. J.*, Vol. 47, No. 8, 2014, pp. 1359–1371, http://dx.doi.org/10.1617/s11527-014-0310-y

[18] Boyer, R. E., "Asphalt Rejuventators 'Fact, or Fable'," Asphalt Institute, Panama City, FL, 2000.

[19] Buenrostro-Gonzalez, E., Groenzin, H., Lira-Galeana, C., and Mullins, O. C., "The Overriding Chemical Principles That Define Asphaltenes," *Energ. Fuels*, Vol. 15, No. 4, 2001, pp. 972–978, http://dx.doi.org/10.1021/ef0100449

[20] Long, R. B., "The Concept of Asphaltenes," American Chemical Society, Washington, DC, 1982.

[21] Karlsson, R. and Isacsson, U., "Material-Related Aspects of Asphalt Recycling—State-of-the-Art," *J. Mater. Civil Eng.*, Vol. 18, No. 1, 2006, pp. 81–92, http://dx.doi.org/10.1061/(ASCE)0899-1561(2006)18:1(81)

[22] Shen, J., Amirkhanian, S., and Miller, J. A., "Effects of Rejuvenating Agents on Superpave Mixtures Containing Reclaimed Asphalt Pavement," *J. Mater. Civil Eng.*, Vol. 19, No. 5, 2007, pp. 376–384, http://dx.doi.org/10.1061/(ASCE)0899-1561(2007)19:5(376)

[23] García, Á., Schlangen, E., and Van de Ven, M., "Properties of Capsules Containing Rejuvenators for Their Use in Asphalt Concrete," *Fuel*, Vol. 90, No. 2, 2010, pp. 583–591, https://doi.org/10.1016/j.fuel.2010.09.033

[24] Nahar, S. N., Qiu, J., Schmets, A., Schlangen, E., Shirazi, M., van de Ven, M., Schitter, G., and Scarpas, A., "Turning Back Time: Rheological and Microstructural Assessment of Rejuvenated Bitumen," *Transportation Research Board 93rd Annual Meeting: Compendium of Papers*, Washington, DC, January 12–16, 2014, Transportation Research Board, Washington, DC.

[25] Brown, E. R., "Preventative Maintenance of Asphalt Concrete Pavements," National Center for Asphalt Technology, Auburn, AL, 1988.

[26] Rostler, F. S. and White, R. M., "Rejuvenation of Asphalt Pavements," Materials Research and Development, Oakland, CA, 1970.

[27] Scofield, L. and Timothy, W. M., "Product Evaluation: Bituminous Pavement Rejuvenator," Arizona Transportation Research Center, Phoenix, AR, 1986.

[28] Shen, J., Amirkhanian, S., and Tang, B., "Effects of Rejuvenator on Performance-Based Properties of Rejuvenated Asphalt Binder and Mixtures," *Constr. Build. Mater.*, Vol. 21, No. 5, 2006, pp. 958–964, https://doi.org/10.1016/j.conbuildmat.2006.03.006

[29] Lin, J., Guo, P., Wan, L., and Wu, S., "Laboratory Investigation of Rejuvenator Seal Materials on Performances of Asphalt Mixtures," *Constr. Build. Mater.*, Vol. 37, 2012, pp. 41–45, https://doi.org/10.1016/j.conbuildmat.2012.07.008

[30] "Evaluation of Rejuvenators for Bituminous Pavements," Technical Report AFCEC-TR-76-3, Air Force Civil Engineering Center, Tyndall Air Force Base, FL, 1976.

[31] ASTM D7313-13, *Standard Test Method for Determining Fracture Energy of Asphalt-Aggregate Mixtures Using the Disk-Shaped Compact Tension Geometry*, ASTM International, West Conshohocken, PA, 2013, www.astm.org

[32] Braham, A. F., Buttlar, W. G., Clyne, T., Marasteanu, M., and Turos, M., "The Effect of Long-Term Laboratory Ageing on Asphalt Concrete Fracture Energy," *J. Assoc. Asphalt Paving Technol.*, Vol. 78, 2009, pp. 417–445.

[33] Geiger, L., "Probability Method for the Determination of Earthquake Epicenters from the Arrival Time Only," *Bull. St. Louis Univ.*, Vol. 8, 1912, pp. 60–71.

[34] McGovern, M., Behnia, B., Buttlar, W. G., and Reis, H., "Concrete Testing: Characterization of Oxidative Ageing in Asphalt Concrete – Part 1: Ultrasonic Velocity and Attenuation Measurements and Acoustic Emission Response Under Thermal Cooling," *Insight*, Vol. 55, No. 11, 2013, pp. 596–604, https://doi.org/10.1784/insi.2012.55.11.596

[35] Leighton, F. and Duvall, W. I., "Least Squares Method for Improving Rock Noise Source Location Techniques," United States Bureau of Mines, Washington, DC, 1972.